FLOOD HAZARD ASSESSMENT USING PANCHROMATIC SATELLITE IMAGERY

Ahmed Shaker a, *, W.Y. Yan a, b, M.S. Wong c, Nagwa El-Ashmawy d, Bahaaeddin IZ Alhaddad e

[a] Department of Civil Engineering, Ryerson University, Canada - ahmed.shaker@ryerson.ca
[b] Planning Department, The Government of the Hong Kong Special Administrative Region – wyyan@pland.gov.hk
[c] Department of Land Surveying and Geo-Informatics, The Hong Kong Polytechnic University, Hong Kong - wongmansing.charles@gmail.com
[d] Regional Center for Training and Water Studies, Ministry of Water Resources and Irrigation - nelashmawy@rctws.com
[e] Centre de Política de Sòl i Valoracions- CPSV, Universitat Politècnica de Catalunya- UPC - bahaa.alhaddad@upc.edu

Commission VI, WG VII/5

KEY WORDS: Flood, Hazard Assessment, Classification, Panchromatic, Texture Analysis

ABSTRACT:

Panchromatic (PAN) satellite imagery has been used successfully in different applications such as topographic mapping and terrain modelling. Nevertheless, PAN imagery is still one of the less used digital sources for land-change studies except few processes where the high-resolution of the PAN images is used to improve the visualization quality of the multi-spectral images. This research aimed to study and facilitate the use of the PAN satellite imagery in image classification for flood hazard assessment application. In particular, this research is investigating the potential use of PAN satellite imagery for flood hazard assessment of one of the high floods of the Nile River occurred in Year 1998. Several existing techniques and approaches used for digital image processing were examined and assessed for PAN image classification. The study focuses on four different approaches that could be used for PAN image classification and flood hazard assessment: a) image interpretation, b) edge detection, c) pixel-based image classification, and d) texture analysis (TEX). The described approaches were investigated for PAN satellite imagery covering a part of the Nile Valley in Egypt. Two SPOT PAN satellite images covering part of the Nile Valley in Egypt before and after the 1997/1998 Nile flood have been utilized. Different areas of interest (islands, coastal areas, etc.) have been identified to study the efficiency of the previous classification approaches for PAN image classification. The results of four PAN image classification approaches are presented and assessed for the study sites using area and sample comparative analysis. The results revealed that Contextual Classifier on PAN imagery and Maximum Likelihood Classifier on TEX imagery offer the nearest estimation of flooding areas. The study shows high integrity of the tested approaches for PAN image classification and accuracy comparable to conventional signature-based classification technique of multi-spectral images could generally be achieved.

1. INTRODUCTION

Several research work have been conducted to explore the usage of PAN imagery in various applications such as road extraction (Duta, 2000), land cover mapping (Narasimha Rao et al., 2002), urban studies (Zhang et al., 2003), and change detection (Phalke and Couloigner, 2005). PAN imagery has finer spatial resolution comparing to the multi-spectral imagery nevertheless, the latter is a superior in image classification due to the availability of different bands in different spectral ranges. Generally, multi-spectral image classification approaches may not be appropriate in classifying PAN imagery. However, introduction of intelligent classification and feature extraction methodologies for PAN imagery including image segmentation (Segl and Kaufmann, 2001), object-oriented classification (Kressler et al., 2003), image morphology (Benediktsson et al., 2003), and Support Vector Machine (Fauvel et al., 2007) are of increasing interest. Adoption of texture analysis is the recent trend for classifying remote sensing imagery and has been shown as a promising method to improve the classification accuracy. Texture analysis takes into consideration the distribution and variation of neighbourhood pixel data and hence the spatial properties of classes could be incorporated as one of the classification criterion to compensate the lack of the spectral information.

Comprehensive literature review of texture analysis in remote sensing science can be found in (Shaban and Dikshit, 2001; Narasimha Rao et al., 2002 and Zhang et al., 2003). Texture analysis can be categorized into structural level and statistical level textures and this study would focus on the latter approach as it is more suitable for classification of natural scenes, especially in satellite imagery (Shaban and Dikshit 2001). In the statistical approach, the stochastic properties of the spatial distribution of grey level (GL) in the image are characterized. The resultant texture measures include statistics of grey level histograms, and autocorrelation and auto regression models (Narasimha Rao et al., 2002). Amongst all popular algorithms, Grey Level Co-occurrence Matrix (GLCM) is the widely adopted one (Haralick et al.1973). First order and second order texture measures on GLCM consists of *Standard Deviation*, *Range*, *Minimum*, *Maximum* and *Mean.* The second order of texture measures includes *Angular Second Moment*, *Contrast*, *Correlation*, *Dissimilarity*, *Entropy*, *Information Measures of Correlation*, *Inverse Difference Moment* and *Sum of Squares Variance* where majority of these could be found in commercial remote sensing software package. Use of the GLCM texture

* Corresponding author. Dr. Ahmed Shaker, Email: ahmed.shaker@ryerson.ca

still require decision on a number of parameters including the spatial resolution, the spectral band, the quantization level of the image, the size of the moving widows, the inter-pixel distance and angle during the co-occurrence computation and the statistics used (Marceau et al 1990).

With the claimed classification accuracy improvement using texture analysis, the study would incorporate the measures with various supervised classification methodologies to detect the Nile discharge area with two panchromatic satellite imagery captured before and after the flood. As a baseline for the comparison, a visual interpretation approach is introduced to delineate the boundary manually and extracted the flooding areas. A semi-automatic method using edge detection method is also introduced. Finally, a comprehensive comparison between these approaches are presented with performance metrics including processing time, visual analysis, classification accuracy and the Nile discharge area.

2. STUDY AREA

The study was conducted in the northern portion of the Nile River in Egypt (29° 16 'N, 31°17' E) as shown in Figure 1. Nile River, regarded as the longest river in the world, is facing flooding problem every year. The river passes through ten different African countries which are affected by the river flood during the rainy seasons. Egypt used to face the Nile flood peacefully after building the Aswan High Dam, South of Egypt. Yet, for the safety of the Aswan High Dam, releasing larger discharge is one of different scenarios that have been adopted to deal with the high floods problem. Other scenarios including flush some of the exceeding water into the western desert. Releasing larger discharge may affect some of the Nile islands, and covering the adjacent areas of the Nile by water. This research is investigating the potential use of PAN satellite imagery for flood hazard assessment of one of the high floods occurred in 1998.

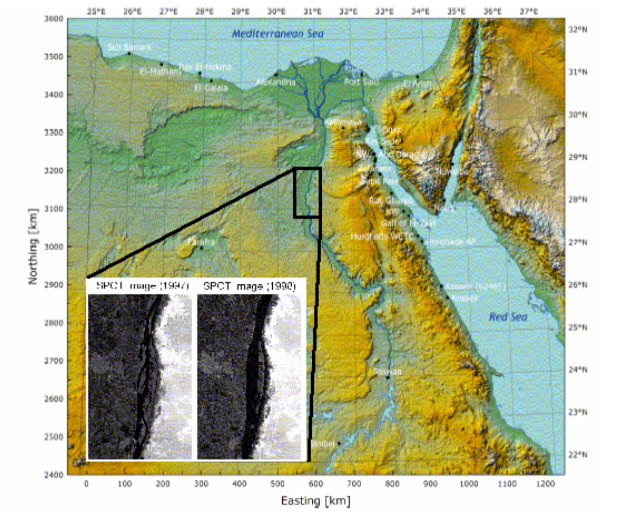

Figure 1. Study Area and SPOT Imagery of Egypt

In this study, two cloud-free SPOT PAN satellite images covering about 6 x 10 km of a part of the Nile Valley before and after the 1997/1998 Nile flood were acquired. The spatial, spectral, and radiometric resolutions of the pair of images are 10m, 0.51-0.73µm, and 8 bit, respectively. Due to the lack of GIS data and digital elevation model, ortho-rectification for the pair of images could not be achieved. However, the geometric distortion can be ignored due to the minimal elevation along the river. Image-to-image registration has been carried out so that an identical image coordinate system could be established for assessment. The overall registration error with 40 reference points was less than 1.5 pixels. Different areas of interest such as islands, the river banks, etc. have been identified. Figure 2 shows the area covered by the SPOT PAN image acquired in year 1997 (before flooding) and 1998 (after flooding).

3. METHODOLOGY

This study focuses on four different approaches that could be used for PAN image classification and flood assessment: a) image interpretation, b) edge detection, c) pixel-based image classification, and d) texture analysis. Concerning the image interpretation, the pair of SPOT images were first imported into ESRI® ArcGIS™ 9.0 for digitizing the boundary of the Nile River before and after the flood. Small islands appeared along the river were delineated, as such the output of the river would be a polygon with holes. After completing image digitization, the GIS polygon layer representing the water zones of the Nile River in 1998 was clipped by the one of 1997. The resulting GIS polygon layer thus represents the flooding zones. . The areas of these zones were calculated for assessing the quality of the other image classification approaches later. The drawback of this methodology is the labour intense and time-consumption, which may take hours for the entire digitization process.

Regarding the above time-consuming process, a semi-automatic process was adopted, which is the edge detection method. Canny edge detection algorithm (Canny, 1986) offers sub-pixel interpolation for detecting edges using a Gaussian filter. The algorithm is based on the computation of the image gradient. Pixels whose gradient are not local maximum are suppressed and an edge strength image is generated. Polylines are then extracted from the edge strength image. These processes could be achieved from PCI Geomatica® EASI Modeller using Lineament Extraction. With a threshold value of 13 for the Gaussian filter amongst various trails, line features were extracted from the pair of PAN imagery automatically (See Figure 2). The line features nearby the Nile River were manually connected to form a new GIS polygon for both images. The flooding areas were extracted by using the polygon clipping approach similar to the case of image interpretation.

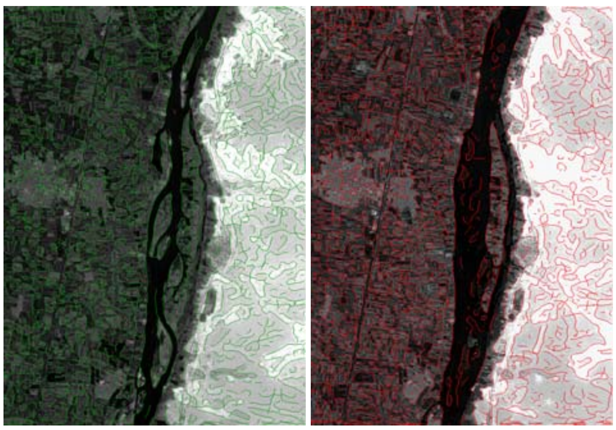

Figure 2. Line Features Extracted from Canny Edge Detector (Left 1997, Right 1998)

A number of research focused on the adoption of texture analysis with different resolution of remote sensing data including 1.1km AVHRR image (Baraldi and Parmiggiani, 1995), 100m ERS-1 SAR image (Soh and Tsatsoulis, 1999), 20m SPOT XS image (Marceau et al, 1990; Shaban and Dikshit, 2001), 10m SPOT PAN image (Zhang et al, 2003), 6m IRS PAN image (Smits and Annoni 1999; Narasimha et al 2002), 1m IKONOS-2 PAN image (Kayitakire et al, 2006), 1m digital orthophoto (St-Louis et al 2006), 0.6m & 2.4m QuickBird image (Wang et al 2004). The significant differences amongst all the studies are the selection of window size, selection of GLCM texture and the problem domain for the classification. With the increase in CPU power and disk storage, the increase of cell size, orientation, inter-pixel distance as well as the quantization level would no longer influence for the data preparation process. The study does not attempt to compare and perform testing to find out an optimal parameter setting; instead we review these literatures and investigate a suitable set of parameters for this application.

According to Marceau et al (1990), and Baraldi and Parmiggiani (1995), the window size for texture analysis should be smaller than the smallest object to be mapped for easy discrimination. As such, 5x5 window size was selected which was able to capture the textural characteristics, especially those small isolated island along the Nile River despite of larger window size (7x7, 9x9) for SPOT image for urban pattern study (Shaban and Dikshit 2001; Zhang et al 2003). Any increase of the window size in these studies was found not statistically significant.

Orientation is less important amongst the parameters of GLCM textures. We adopted θ = 0°, 45°, 90° and 135°, which could already cover all directions of Nile River and its islands in the PAN imagery. This setting was also adopted in most of the literature. Increase or uncertain series of orientation of were only appropriate for accommodation of systematic spatial patterns based on orientation with the image (Soh and Tsatsoulis, 1999).

The inter-pixel distance was set to be 1 in this study as there was no significant difference from 1 to 8 in Soh and Tsatsoulis's (1999) and from 1-4 in Shaban and Dikshit (2001)'s. Higher inter-pixel distance may even decrease the overall classification accuracy in their findings.

According to Soh and Tsatsoulis's (1999), the more quantization schemes could smooth an image and thus reduced noise-induced effects to some degree. With no constraint in data storage, we set 32 quantization levels for the image, which was already enough comparing with Shaban and Dikshit's (2001) study. As the computation power and disk storage was no longer a constraint in this study, the quantization level would not be linearly rescaled for enhancing the classification performance.

Selection of GLCM texture is a critical factor affecting the classification accuracy. Incorporation of excessive texture would degrade the performance and has been proven in literature (Shaban and Dikshit 2001 and Zhang et al 2003). Regarding the problem domain and the spectral information, incorporation of two to four texture measures were optimal in these researches. The remaining issue would be the selection of appropriate texture. With the conclusion from Zhang et al (2003), *Mean* combined with another GLCM texture feature produced the best result amongst all combinations of two GLCM texture. *Contrast* could also provide the high classification accuracy in Shaban and Dikshit's (2001) testing. Following the recommendation from Hall-Beyer's (2007) experience on texture analysis, *Standard Deviation* was added to form two texture measures for "descriptive statistics" group in addition to *Mean*. As there were already two first order GLCM texture, one second order GLCM texture *Dissimilarity* was added to enhance the heterogeneity of the Nile River from the grey level of the nearby agricultural land. The equation of Dissimilarity, Contrast, Mean and Standard Deviation are presented as bellows:-

$$Contrast = \sum_{i=0}^{N-1}\sum_{j=0}^{N-1} P_{i,j}(i-j)^2 \quad (1)$$

$$Dis = \sum_{i=0}^{N-1}\sum_{j=0}^{N-1} P_{i,j}|i-j| \quad (2)$$

$$Mean = \mu = \sum_{i=0}^{N-1}\sum_{j=0}^{N-1} iP_{i,j} \quad (3)$$

$$SD = \sqrt{\sum_{i=0}^{N-1}\sum_{j=0}^{N-1} P_{i,j}(i-\mu)^2} \quad (4)$$

where N = number of grey levels
P = normalized symmetric GLCM of dimension N x N
$P_{i,j}$= is the (i , j)th element of P

Supervised image classifications were carried out in PCI Geomatica® 10.1. Training sites in polygon were identified with three different land cover classes: Agricultural Land (Class 1), Desert Area (Class 2) and Water Bodies (Class 3) with large seperability (> 1.9) in Bhattacharya Distance. Figure 3 shows the training samples of these three land cover classes. Five supervised classification methodologies were introduced to classify the three stated classes. Parametric classifiers including Minimum Distance (MinD) and Maximum Likelihood (MLC) and non-parametric classifiers including Artificial Neutral Network (ANN) Classifier, Contextual (CON) Classifier and 5-Nearest Neighbour (kNN) Classifier were adopted to classify the two PAN images using the same training samples. The classification accuracy was then evaluated with 500 random samples. Finally, image subtraction was carried out to dig out the flooding zones from the two classified results. Three rounds of classification were carried out (PAN imagery only, TEX only, and incorporation of PAN and TEX imagery) to compare the accuracy and the final computed flooding areas.

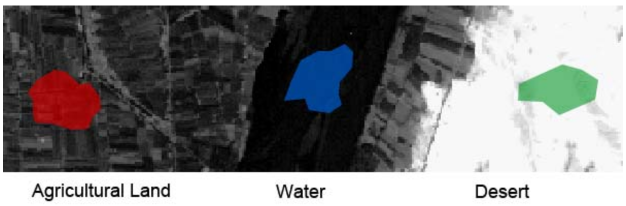

Figure 3. Samples of Land Cover Classes in SPOT PAN Imagery

4. RESULT AND DISCUSSION

Results from the four different approaches for PAN image classification are presented for analysis. We compared the results of these approaches based on four performance metrics: time, visual quality, flooding areas and sample-based accuracy assessment. Undoubtedly, the most time-consuming method is the image interpretation method. It takes more than two hours to digitize the river boundaries for the pair of the images (6x10 km). The time would significantly increase if the study area is extended and contains many islands along the river. Edge detection method is quicker; whilst the manual process to connect the line segments requires more than one hour. As such, edge detection would be the second time consuming process. The image classification approach only requires less than an hour; texture analysis is also quick regarding the increase of CPU power if the window size and the image size are not large. The cost and manpower requirements are significantly lower using automatic image classification with or without texture analysis.

Figures 4a through 4q show extracts of the flooding areas derived from various approaches as aforementioned. The majority of the results match the geometry and appearance of the flooding zones derived from image interpretation. However, the kNN classifier applied on PAN imagery only (Figure 4c) generated a speckled scattering pixel which appear noisy comparing with other results. The Canny edge detector (Figure 4p) generated curvy and discontinuous features and indicated a severe loss of image detail. Finally, it is surprising that the MLC with PAN and TEX (Figure 4o) generated more flooding areas in the lower part of the river and it is totally diverse with all other results. Apart from these three methods, the difference between the results of the remaining methods could not be distinguished in terms of visual analysis and hence the accuracy assessment and the computed flooding areas would be the critical factors for assessment.

Table 1 shows the result of the computed flooding areas derived from various image classification methods with inclusion of the three datasets: PAN image only, four texture channels, and PAN with four texture channels, respectively. The area delineated by visual interpretation method (29208 units square) is regarded as the reference for the comparison. Table 2 shows the difference in percentage of each method comparing to the visual interpretation result. The area derived from Canny edge detector is 22789 unit square, which is the smallest calculated area and 22% less than the reference. In terms of classification methods, MLC seems to be superior to others as the area derived with the three data sets are very close to that from the visual interpretation. kNN's result is significantly improved with the inclusion by texture (32% improvement); however, all the result derived from the three datasets are still unacceptable. MinD and ANN classifier produced the poorest result amongst the three datasets. CON classifier produced a very close result with PAN imagery only; however, the flooding areas derived from texture dataset only is significantly increased and then dropped to the mean value for the combination dataset with PAN and TEX. This could be explained by the rationale of contextual classifier which includes the spatial context from neighbourhood pixels. This is more or less as what texture analysis achieved. Therefore the effect of CON classifier on PAN imagery is similar as the result of MLC classifier on TEX channels. In terms of datasets, supervised classification with only texture channels performs better than those with inclusion of PAN imagery with TEX except the result derived from CON classifier which has been explained by the classifier's principle. This phenomenon is also applied when comparing with TEX and PAN imagery.

	PAN	**TEX**	**PAN+TEX**
ANN	34715 (4)	32327 (2)	33759 (4)
CON	30226 (1)	36259 (5)	33242 (3)
kNN	42049 (5)	32831 (3)	32816 (2)
MinD	34117 (3)	34560 (4)	35989 (5)
MLC	26305 (2)	29917 (1)	30434 (1)

* Bracket number means the ranking of the closest area comparing with the visual interpretation.

Table 1. Flooding Area due to Nile Discharge in Unit Square

	PAN	**TEX**	**PAN+TEX**
ANN	+19%	+11%	+16%
CON	+3%	+24%	+14%
kNN	+44%	+12%	+12%
MinD	+17%	+18%	+23%
MLC	-10%	+2%	+4%

Table 2. Area Difference Comparing with Visual Interpretation in Percentage

The kappa statistics of individual land cover classes and overall accuracy obtained from the classification with inclusion of PAN image only, four texture channels, and both PAN and texture channels are presented in Table 3. The Bhattacharya Distance were examined with value larger than 1.9 before classification in those three datasets, the three classes were claimed to be highly heterogeneous with clear delineation amongst the class boundaries. As such, the problem of between-class spectral confusion and within-class spectral variation should not be occurred in this study. The overall accuracy are within 80% to 90% for the SPOT 1997 imagery and over 90% for the SPOT 1998 in most of the cases. None of the classifiers are superior in all the three data sets, but the relative ranking amongst the three data sets are similar in both 1997 and 1998 imagery. However, the parametric classifier MinD and MLC performed the worst in texture classification where this phenomenon aligns with Shaban and Dikshit's study (2001) in urban environment. All classifiers produced their highest overall accuracy with PAN and TEX in SPOT 1997 imagery and PAN only in SPOT 1998 imagery. In terms of land cover class, the kappa statistics of agricultural land, desert and water bodies are around 0.6, 0.9 and 1.0 respectively and they are in ascending order in most of the results; except all the results derived from MinD. Special case like MinD classification of SPOT 1998 PAN imagery is even inverted. With the low kappa statistics, especially in water bodies, result generated from MinD classifier is unreliable in this study regarding the heterogeneous classes.

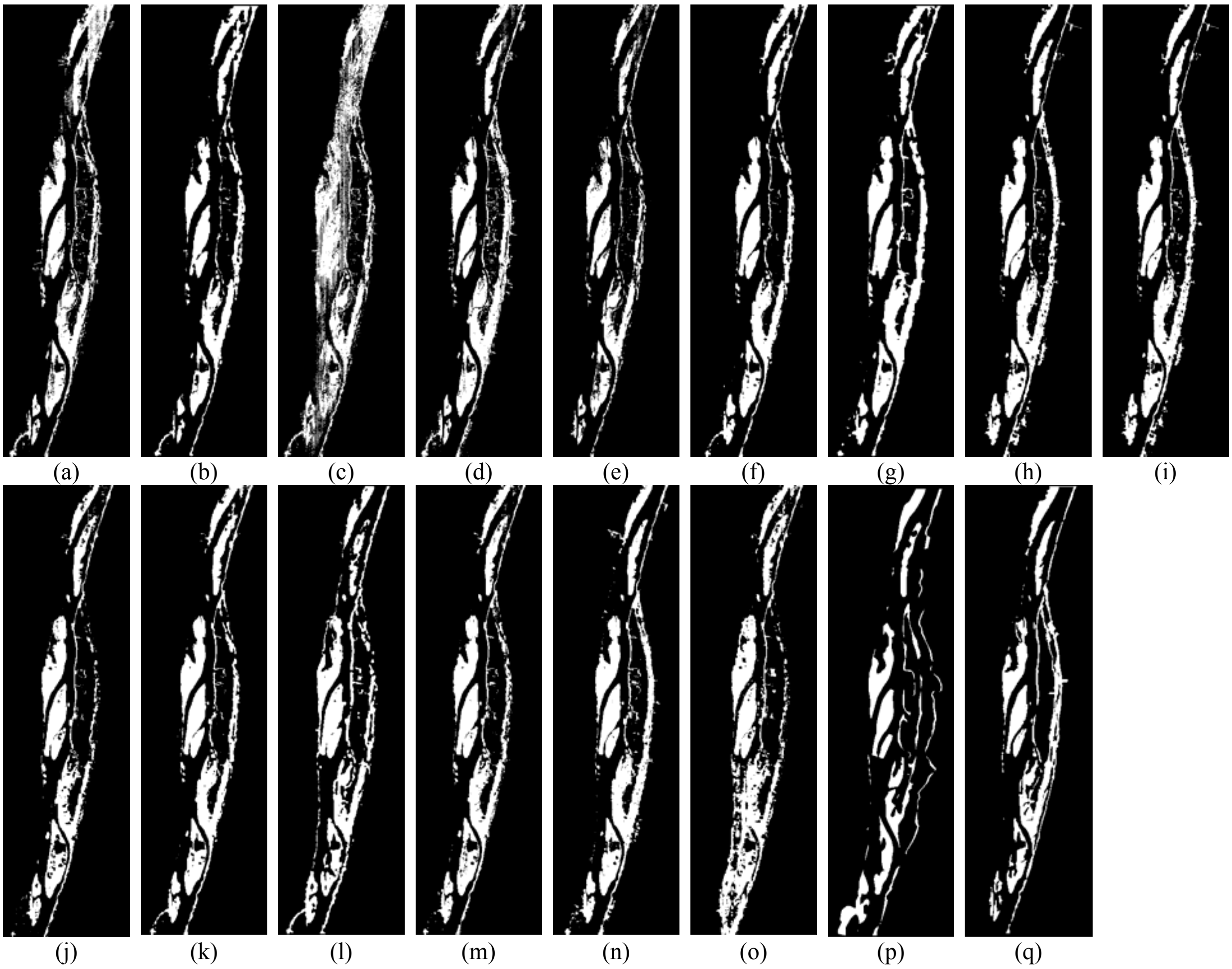

Figure 4. Classification Result of PAN Imagery using (a) ANN, (b) CON, (c) kNN, (d) MinD and (e) MLC; Classification Result of TEX Imagery using (f) ANN, (g) CON, (h) kNN, (i) MinD and (j) MLC; Classification Result of PAN+TEX Imagery using (k) ANN, (l) CON, (m) kNN, (n) MinD and (o) MLC; Result derived from Canny edge detection algorithm (p) and Result derived from Image Interpretation (q)

	SPOT 1997				**SPOT 1998**			
	Agricultural Land	Desert	Water Bodies	Overall Accuracy	Agricultural Land	Desert	Water Bodies	Overall Accuracy
PAN (ANN)	0.6278	0.9078	1.0000	86.8% (3)	0.9137	0.9562	0.9686	96.4% (1)
PAN (CON)	0.6430	0.9220	0.9090	86.2% (4)	0.7788	0.9552	0.9795	91.6% (4)
PAN (kNN)	0.5383	0.9734	1.0000	84.4% (5)	0.7901	0.9648	1.0000	93.4% (3)
PAN (MinD)	0.7526	0.9821	0.9794	92.4% (1)	0.9909	0.9646	0.7026	93.4% (3)
PAN (MLC)	0.7615	0.8922	0.9794	90.8% (2)	0.8217	0.9478	1.0000	94.0% (2)
TEX (ANN)	0.6592	0.9318	1.0000	88.4%(1)	0.7844	0.9731	1.0000	93.4% (1)
TEX (CON)	0.6027	0.9462	1.0000	85.6% (2)	0.7247	0.9901	0.9616	90.4% (3)
TEX (kNN)	0.6183	0.8547	1.0000	85.4% (3)	0.7337	0.9635	1.0000	91.6% (2)
TEX (MinD)	0.6546	0.6445	0.8766	80.6% (4)	0.7104	0.7598	0.7011	83.2% (5)
TEX (MLC)	0.5438	0.6663	1.0000	78.6% (5)	0.6695	0.9623	1.0000	89.4% (4)
PAN+TEX (ANN)	0.6585	0.9651	1.0000	89.0% (2)	0.7901	0.9646	1.0000	93.4% (2)
PAN+TEX (CON)	0.7152	0.9729	0.8297	88.8% (3)	0.7167	0.9641	0.9748	89.8% (5)
PAN+TEX (kNN)	0.6381	0.9734	1.0000	88.4% (4)	0.7709	0.9648	1.0000	92.8% (3)
PAN+TEX (MinD)	0.7243	0.9822	0.8954	90.8% (1)	0.8522	0.9646	0.8585	93.6% (1)
PAN+TEX (MLC)	0.6063	0.9078	1.0000	86.0% (5)	0.7217	0.9641	1.0000	91.2% (4)

Table 3. Kappa Statistics of Three Land Cover Classes and Overall Accuracy

5. CONCLUSION

This paper discusses the potential use of PAN satellite imagery for flood hazard assessment by using different classification techniques. Four image classification techniques have been studied including classification by visual interpretation, edge detection, pixel-based image classification, and pixel-based image classification with texture analysis. Two PAN images of SPOT 4 satellite, captured in 1997 and 1998 (before and after flood), covering a part of the Nile River and its valley were adopted in this study. Sample and area comparative analysis were held to assess the potential accuracy achieved from the different image classification techniques.

The results and the analysis reveal that: firstly, the visual image interpretation and the Canny edge detection approach are not efficient in terms of processing time. However, visual image interpretation is the most accurate technique and Canny edge detection may not accurate enough to compute the flooding areas. To meet the requirement for the area computation of the flooding areas, it was found that CON classifier on PAN imagery, and MLC on purely TEX imagery produced the closest result to the visual interpretation. Although the overall accuracy in these two methods for the images captured in 1997 and 1998 are comparably low, the kappa statistics of water bodies and the overall accuracy are still high enough to be accepted. With these highly heterogeneous land cover class, inclusion of texture may not enhance the classification performance and classification of PAN imagery was sufficient to delineate the flooding areas.

REFERENCE

Baraldi, A., and Parmiggiani, F., 1995. An Investigation of the Textural Characteristics Associated with Gray Level Cooccurrence Matrix Statistical Parameters. *IEEE Transactions on Geoscience and Remote Sensing*, 33(2), pp. 293-304.

Benediktsson, J.A., Pesaresi, M., and Arnason, K., 2003. Classification and Feature Extraction for Remote Sensing Images From Urban Areas Based on Morphological Transformations. *IEEE Transactions on Geoscience and Remote Sensing*, 41(9), pp. 1940-1949.

Canny, J.F., 1986. A computational approach to edge detection. *IEEE Transactions on Pattern Analysis & Machine Intelligence*, 8(6), pp. 679-698.

Duta, N., 2000. Road Detection in Panchromatic SPOT Satellite Images. *Proceedings of 15th International Conference on Pattern Recognition*, Vol.4, pp. 308-311.

Franklin, S.E., Wulder, M.A., Gerylo, G.R. 2001. Texture analysis of IKONOS panchromatic data for Douglas-fir forest age class separability in British Columbia. *International Journal of Remote Sensing*, 22(13), pp. 2627-2632.

Hall-Beyer, M., 2007. The GLCM Tutorial Home Page, University of Calgary, Canada, http://www.fp.ucalgary.ca/mhallbey/tutorial.htm (accessed 17 Feb. 2008)

Kayitakire, F., Hamel, C., and Defourny, P., 2006. Retrieving Forest Structure Variables based on Image Texture Analysis and IKONOS-2 Imagery. *Remote Sensing of Environment*, Vol. 102, pp, 390-401.

Kressler, F.P., Kim, Y.S., and Steinnocher, K.T., 2003. Object-oriented Land Cover Classification of Panchromatic KOMPSAT-1 and SPOT-5 Data. *Proceedings of IEEE International Geosciences and Remote Sensing Symposium 2003*, pp. 3471-3473.

Marceau, D.J., Howarth, P.J., Dubois, J-M. M. and Gratton, D.J. 1990. Evaluation of the Grey-Level Co-Occurrence Matrix Method for Land Cover Classification using SPOT Imagery. *IEEE Transactions Geoscience and Remote Sensing*, 28(4), pp. 513-519.

Narasimha Rao, P.V., Sesha Sai, M.V.R., Sreenivas, K., Krishna Rao, M.V., Rao, B.R.M., Dwivedi, R.S., and Venkataratnam, L., 2002. Textural Analysis of IRS-1D Panchromatic Data for Land Cover Classification. *International Journal of Remote Sensing*, 23(17), pp. 3327-3345.

Phalke, S.M., and Couloigne,r I., 2005. Change Detection of Linear Man-made Objects using Feature Extraction Technique. Proceedings of the 13th *International Conference on GeoInformatics*, 17-19 August 2005, Toronto, Canada.

Segl, K., and Kaufmann, H., 2001. Detection of Small Objects from High Resolution Panchromatic Satellite Imagery based on Supervised Image Segmentation. *IEEE Transactions on Geoscience and Remote Sensing,* 39(9), pp. 2080-2083.

Shaban, M.A., and Dikshit, O., 2001. Improvement of Classification in Urban areas by the Use of Textural Features the Case Study of Lucknow City, Uttar Pradesh. *International Journal of Remote Sensing*, 22(4), pp. 565-593.

Smits, P.C. and Annoni, A., 1999. Updating Land-Cover Maps by Using Texture Information from Very High-Resolution Space-Borne Imagery. *IEEE Transactions on Geoscience and Remote Sensing*, 37(3), pp. 1244-1254.

Soh, L.K., and Tsatsoulis, C., 1999. Texture Analysis of SAR Sea Ice Imagery using Gray Level Co-occurrence Matrices. *IEEE Transactions on Geoscience and Remote Sensing*, 37(2), pp. 780-795.

St-Louis, V., Pidgeon, A.M., Radeloff, V.C., Hawbaker, T.J., and Clayton, M.L., 2006. High-resolution Image Texture as a Predictor of Bird Species Richness. *Remote Sensing of Environment*, 2006(105), pp. 299-312.

Wang, L., Sousa, W.P., Gong, P., and Biging, G.S., 2004. Comparison of IKONOS and QuickBird Images for Mapping Mangrove Species on the Caribbean Coast of Panama. *Remote Sensing of Environment*, 2004(91), pp. 432-440.

Zhang, Q., Wang, J., Gong, P., and Shi, P., 2003. Study of Urban Spatial Patterns from SPOT Panchromatic Imagery using Textural Analysis. *International Journal of Remote Sensing*, 24(21), pp. 4137-4160.